# Realization of DC–DC Buck Converter Based on Hybrid $H_2$ Model Following Control

J. S. Fang, Sheng-Hong Tsai, Jun-Juh Yan, P. L. Chen, and Shu-Mei Guo, *Member, IEEE*

***Abstract*—The buck converter is frequently introduced in the industry to maintain the stability of the voltage output when having the interference suddenly. In order to promote the robustness of the buck converter, a novel hybrid $H_2$ model following control (HHMFC) is developed based on digital redesign sliding mode control in this article. First, we design $H_2$ model following SMC in the continue-time domain. Then, by using the digital redesign approach, the continuous SMC is redesigned to a corresponding discrete-time SMC and the proposed HHMFC is achieved. Finally, we apply the developed HHMFC to realize a robust buck converter. With both the simulation and experiment results, we can conclude that the proposed HHMFC can easily and successfully apply to the practical realization for the buck converter with better robustness performance.**

***Index Terms*—Buck converter, digital redesign, hybrid model following control, robustness, sliding mode control (SMC).**

## I. Introduction

SWITCH-MODE direct current–direct current (dc–dc) converters transfer the dc voltage level to another, which may be higher or lower, by storing the input energy temporarily and releasing that energy to the output at a different voltage. In this article, the buck converter discussed is a step-down converter that reduces the input voltage to the output voltage. This type of buck converters is used widely in engineering applications, such as photovoltaic systems [1], electrical vehicles [2], etc. However, since the performance of a buck converter is always influenced by the different disturbances, such as the parameter variations, measurement error, etc., the most important issue of the buck converter is the robust stability with the instant disturbance. Thus, in the literature, many works with different design approaches explored the stability of the buck converter, such as sliding mode control (SMC) [3]–[5], fuzzy control [6], [7], adaptive control [8], adaptive-predictive control [9], back stepping control [10], etc. In this article, we aim to propose a novel hybrid $H_2$ model following control (HHMFC) based on digital redesign SMC to implement the buck converter. To make sure the stability in the sampled-data uncertain system, we introduce the model following control theory. By setting a model system as the desired reference model, we design the model following control to obtain desired trajectories for the controlled buck converter. However, using the traditional model following control cannot effectively repress the unknown disturbances and uncertain model. Therefore, many papers propose different robust control methods to cope with these problems [11], [12].

Recently, SMC has been successfully applied to depress the disturbances. In connection with SMC, there are many applications [13]–[15]. The work [13] proposed an integral SMC algorithm to process the changeable switching frequency problem in converters. The work [14] used a robust neuro-fuzzy-SMC with extended state observer to constrain the disturbance. The report [15] introduced an adaptive nonconventional SMC to solve an inequality constrains. Thus, according to the research works in the literature, SMC is able to efficiently suppress disturbances. On the other hand, for better reliability, lower cost, smaller size, more flexibility, and better performance, it is a current trend by using digital microcontroller chips to implement control solutions. However, to utilize the digital signal processing microcontroller to implement the control schemes, the traditional continuous-time SMC design methods proposed in [13]–[15] are not applicable. We must discuss discrete SMC in the discrete-time domain [16]–[18]. In the works [19], [20], the papers indicated that we first need to choose the proper switching surface function for the discrete-time system and discuss the dynamics of the discrete-time system. However, it is very difficult to analyze and design the digital controller in the discrete-time domain, especially for the hybrid controlled systems. In this article, to solve this problem, the digital-redesign method is proposed to directly transform the well-designed continuous analog controller to the discrete type. This proposed design procedure not only can easily obtain a discrete-time HHMFC but also guarantee the robust performance even if the system is with perturbations. Therefore, the discrete HHMFC proposed in this article is easy to implement by using a digital microprocessor controller. First, we design the continuous model following SMC in the continue-time domain. Then, we transfer the continuous

Manuscript received August 31, 2020; revised December 13, 2020 and January 28, 2021; accepted February 14, 2021. Date of publication March 3, 2021; date of current version October 27, 2021. This work was supported by the Ministry of Science and Technology, Taiwan, under MOST 108-2221-E-006-213-MY3 and MOST-109-2221-E-167-017. (*Corresponding author: Jun-Juh Yan.*)

J. S. Fang, Sheng-Hong Tsai, and P. L. Chen are with the Department of Electrical Engineering, National Cheng-Kung University, Tainan 701, Taiwan (e-mail: fjshow611@gmail.com; shtsai@mail.ncku.edu.tw; affectionate1019@gmail.com).

Jun-Juh Yan is with the Department of Electronic Engineering, National Chin-Yi University of Technology, Taichung 41107, Taiwan (e-mail: jjyan@ncut.edu.tw).

Shu-Mei Guo is with the Department of Computer Science and Information Engineering, National Cheng-Kung University, Tainan 701, Taiwan (e-mail: guosm@mail.ncku.edu.tw).

Color versions of one or more figures in this article are available at https://doi.org/10.1109/TIE.2021.3062268.

Digital Object Identifier 10.1109/TIE.2021.3062268

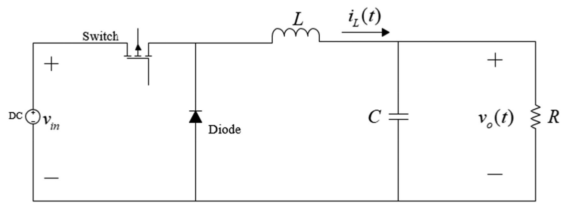


Fig. 1. Circuit structure of the buck converter.

SMC to discrete-time SMC by using the digital redesign technology. The digital redesign approach is a method for directly transferring the continuous-time controller to a discrete-time controller [21], [22]. Based on the digital redesign theorem, we can discretize the predesigned continuous model following SMC to discrete-time SMC based on the Euler approach. Besides, to suppress the disturbances, we also combine SMC with the linear quadratic analog tracker (LQAT). With the Euler approach, we ensure the sliding mode function can converge to zero in finite time and the hitting condition is satisfied in the discrete-time domain. As mentioned above, we can easily design and realize the robust digital HHMFC which has not been discussed in the literature. Since it is easy to analyze and implement, HHMFC is worth exploring in the future. It is worth to note that the traditional SMC uses the sign function to design the sliding manifold, but it causes chattering phenomenon in the input. To suppress the chattering phenomenon, we replace sign function by the saturation function [19], so we can solve this problem. Furthermore, we apply the developed HHMFC to the buck converter with SIMULINK simulation. Then, we implement the HHMFC on the buck converter by using the Raspberry Pi. With both the simulation and experiment results, we can conclude that the proposed HHMFC can easily and successfully apply to the practical realization for the buck converter with better robustness performance.

In this article, we denote the transport for a matrix $w$ by $w^T$. $\|w\|$ is used to denote the Euclidean norm of the vector $w$. $I_n \in \Re^{n\times n}$ represents the identity matrix. $|w|$ is the absolute value for a constant $w$. $w^\dagger = (w^T w)^{-1} w^T$ denotes to the pseudo inverse matrix for a matrix $w \in \Re^{n\times m}$ and $w^\dagger w = I_m$. $\mathrm{sgn}(w)$ is the nonlinear sign function of $w$ and if $w > 0$, we have $\mathrm{sgn}(w) = 1$; if $w < 0$, $\mathrm{sgn}(w) = -1$and $\mathrm{sgn}(w) = 0$ if $w = 0$.

## II. Description of Buck Converter

Fig. 1 presents the general circuit of the dc–dc buck converter. In the circuit, $R$, $L$, and $C$ are the load resistance, inductor, and capacitor, respectively. While $i_L(t)$, $v_{in}$, and $v_o(t)$represent, respectively, the inductor current, applied input voltage, and corresponding output voltage.

Now, we calculate the dynamic model by the Kirchhoff's laws as below. When the switch is ON, the dynamics of the buck converter can be presented as

$$\frac{dv_o(t)}{dt} = \frac{1}{C_0}\left(i_L(t) - \frac{v_o(t)}{R_0}\right) \tag{1.a}$$

$$\frac{di_L(t)}{dt} = \frac{1}{L_0}(v_{in_0} - v_o(t)) \tag{1.b}$$

where $R_0, L_0, C_0$, and $v_{in_0}$, which are the optimal values of load resistance, inductor, capacitor, and input voltage, respectively. When the switch is turned OFF, it will be

$$\frac{dv_o(t)}{dt} = \frac{1}{C_0}(i_L(t) - \frac{v_o(t)}{R_0}) \tag{2.a}$$

$$\frac{di_L(t)}{dt} = -\frac{v_o(t)}{L_0}. \tag{2.b}$$

And then, combining (1) and (2), we get

$$\frac{dv_o(t)}{dt} = \frac{1}{C_0}\left(i_L(t) - \frac{v_o(t)}{R_0}\right) \tag{3.a}$$

$$\frac{di_L(t)}{dt} = \frac{1}{L_0}(\mu v_{in_0} - v_o(t)) \tag{3.b}$$

where $\mu$ is the switch, which means "1" and "0" when the switch state is ON and OFF. Thus, we will propose the control law to decide the switch state is ON or OFF. And the control law will be discussed afterward and the buck converter is supposed to manipulate at continuous-conduction mode.

While measuring the inductor current $i_L(t)$ for (3.b), we need to use the Hall element and it might be disturbed by external noises. Thus, it results in poor accuracy of the current sensor. To overcome this problem, we need to use another method to describe the dynamics of the buck converter. First, we compute the second-order differential of the output voltage as follows:

$$\frac{d^2v_o(t)}{dt^2} = \frac{1}{C_0}\left(\frac{di_L(t)}{dt} - \frac{1}{R_0}\frac{dv_o(t)}{dt}\right). \tag{4}$$

Substitute (3.b) into (4), then we have

$$\frac{d^2v_o(t)}{dt^2} = \frac{1}{C_0}(-\frac{v_o(t)}{L_0} - \frac{1}{R_0}\frac{dv_o(t)}{dt}) + \frac{\mu v_{in_0}(t)}{C_0 L_0}. \tag{5}$$

According to (5), we can solve the problem of the measurement error of current sensors. Then, the state-space equation of the considered buck converter can be represented as follows:

$$\begin{bmatrix}\dot{v}_o(t)\\ \ddot{v}_o(t)\end{bmatrix} = \begin{bmatrix}0 & 1\\ \frac{-1}{C_0L_0} & \frac{-1}{C_0R_0}\end{bmatrix}\begin{bmatrix}v_o(t)\\ \dot{v}_o(t)\end{bmatrix} + \begin{bmatrix}0\\ \frac{v_{in_0}}{C_0L_0}\end{bmatrix}\mu \tag{6.a}$$

$$v_o(t) = \begin{bmatrix}1 & 0\end{bmatrix}\begin{bmatrix}v_o(t)\\ \dot{v}_o(t)\end{bmatrix}. \tag{6.b}$$

With (6.a) and (6.b), it reveals that the state-space equations are only affected by $v_o(t)$. Therefore, one can only use the voltage sensor to measure the output voltage $v_o(t)$. However, we still need to consider the parameters with uncertainties. Therefore, the system dynamics subjected to uncertainties can be described as follows:

$$\begin{bmatrix}\dot{v}_o(t)\\ \ddot{v}_o(t)\end{bmatrix} = \begin{bmatrix}0 & 1\\ \frac{-1}{C_0L_0} & \frac{-1}{C_0R_0}\end{bmatrix}\begin{bmatrix}v_o(t)\\ \dot{v}_o(t)\end{bmatrix} + \begin{bmatrix}0\\ \frac{v_{in_0}}{C_0L_0}\end{bmatrix}\mu + d(x(t),t) \tag{7.a}$$

$$v_o(t) = \begin{bmatrix}1 & 0\end{bmatrix}\begin{bmatrix}v_o(t)\\ \dot{v}_o(t)\end{bmatrix} \tag{7.b}$$

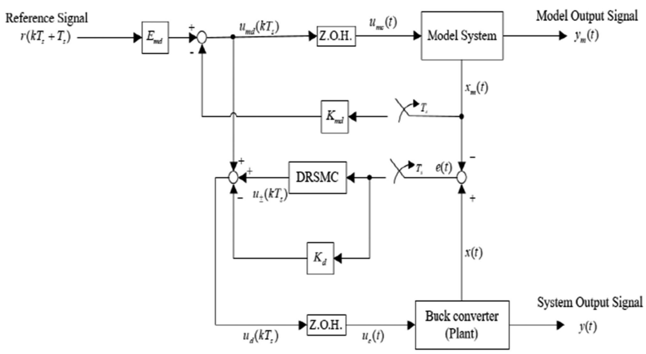


Fig. 2. Hybrid improved model-following controlled system structure for the buck converter.

where $x(t)=[\,v_o(t)\ \dot{v}_o(t)\,]^T$, and $d(x(t),t)$ is the lumped disturbance, which is constituted of the parameter variations. Thus, $d(x(t),t)$ can be described by

$$d(x(t),t)=\begin{bmatrix}0 & 0\\ 0 & \frac{1}{C_0R_0}-\frac{1}{\rho R_0 C_0}\end{bmatrix}x(t) \tag{8}$$

where $\rho R_0$ is the practical load resistance and $\rho\in(0,1)$. As mentioned above, we have derived the state space of the buck converter. In the next section, we continue to design the controller for the buck converter.

## III. Problem Description

The model following controlled system in Fig. 2 has two subsystems including the controlled system and the model system. In this section, we discuss the controller of the buck converter with the hybrid model following control design. We use a digital HHMFC to control a continuous-time buck converter circuit and ensure the output signal of the controlled buck converter can track the states and desired reference signals given in the model system. One can find the digital-redesign sliding mode controller (DRSMC) in Fig. 2 is proposed to control the continuous-time system. By the way, one also designs $E_{md}$ and $K_{md}$ to make sure that the model system output can track the reference signal. However, one uses the digital controller to control the continuous-time system. Therefore, we must apply Z.O.H. to transfer the discrete-time signal to the continuous-time signal.

In Fig. 2, the controlled buck converter is described as

$$\dot{x}(t)=Ax(t)+Bu_c(t)+d(x(t),t) \tag{9.a}$$

$$y(t)=Cx(t) \tag{9.b}$$

where $A\in\Re^{2\times 2}$, $B\in\Re^{2\times 1}$, and $C\in\Re^{1\times 2}$ are the system matrices; $x(t)\in\Re^{2\times 1}$, $u_c(t)\in\Re$, $y(t)\in\Re$, and $d(x(t),t)\in\Re^{2\times 1}$ are the system state vector, the system input vector, the system output vector, the unknown internal nonlinear disturbance, respectively. Besides the unknown internal nonlinear disturbance is assumed to be bounded such that $\|d(x(t),t)\|d\lambda_1\|x(t)\|$ is satisfied.

Now, define the model system as follows:

$$\dot{x}_m(t)=Ax_m(t)+Bu_{mc}(t) \tag{10.a}$$

$$y_m(t)=Cx_m(t) \tag{10.b}$$

where $x_m(t)\in\Re^{2\times 1}$, $u_{mc}(t)\in\Re$, and $y_m(t)\in\Re$ are the model system state vector, the model system input vector, and the model system output vector, individually. We first design the control law of the model system as below

$$u_{mc}(t)=-K_{mc}x_m(t)+E_{mc}r(t) \tag{11}$$

where $K_{mc}$ is the feedback control gain, $E_{mc}$ is the forward control gain, and $r(t)\in\Re$ is the desired reference trajectory. Without loss of generality, we assume the matrices $A$ and $B$ in (7.a) are

$A=\begin{bmatrix}0 & 1\\ \alpha_1 & \alpha_2\end{bmatrix}$, and $B=\begin{bmatrix}0\\ \beta_1\end{bmatrix}$.

Then, we define $K_{mc}$ as

$$K_{mc}=K_{mc1}+K_{mc2} \tag{12}$$

where $K_{mc2}=\beta_1^{-1}[\alpha_1\ \alpha_2]$. Before calculating $K_{mc1}$, one needs to rewrite the model system (10). According to (11), (12), one can obtain $u_{mc}(t)$ as follows:

$$u_{mc}(t)=-\left(K_{mc1}+K_{mc2}\right)x_m(t)+E_{mc}r(t). \tag{13}$$

Substitute (13) into (10), so that we can get

$$\dot{x}_m(t)=\bar{A}x_m(t)+B\bar{u}_{mc}(t) \tag{14.a}$$

$$y_m(t)=Cx_m(t) \tag{14.b}$$

where $\bar{A}=A-BK_{mc2}$ and $\bar{u}_{mc}(t)=-K_{mc1}x_m(t)+E_{mc}r(t)$. Here, the controller gain $K_{mc1}$ can be calculated by using the final-value theorem [23]. After controller gain $K_{mc1}$ is found by using the pole-placement method, the forward gain $E_{mc}$ can be calculated as $E_{mc}=[-C(A-BK_{mc})^{-1}B]^{\dagger}$.

*Remark 1:* The forward gain can be computed by the Final-value theorem. With the Laplace transform, (10.a) and (10.b) can be

$$X_m(s)=[sI-(A-BK_{mc})]^{-1}(BE_{mc}R(s)/s) \tag{15.a}$$

$$Y_m(s)=CX_m(s). \tag{15.b}$$

Then, one can get

$$Y_m(s)=C[sI-(A-BK_{mc})]^{-1}(BE_{mc}R(s)/s). \tag{16}$$

By using the Final-value theorem, the following tracking error can be computed as follows:

$$y_m(\infty)-r(\infty)=\lim_{s\to 0}sY_m(s)-\lim_{s\to 0}sR(s)=0. \tag{17}$$

Define $y_m(\infty)$ and $r(\infty)$ as

$$y_m(\infty)=\lim_{s\to 0}sY(s)=C[-(A-BK_{mc})]^{-1}BE_{mc}R(s) \tag{18}$$

and

$$r(\infty)=\lim_{s\to 0}s(R(s)/s)=R(s). \tag{19}$$

Then, satisfying the following condition $y_m(\infty)=r(\infty)$, we can get $E_{mc}=[-C(A-BK_{mc})^{-1}B]^{\dagger}$. □

## IV. Digital-Redesign-Based SMC Design

As mentioned in the Introduction, we will first design the SMC in the continuous-time domain. Then, we use the digital redesign approach to discretize the obtained continuous-time SMC to be a discrete-time SMC.

### A. Improved Continuous-Time $H_2$ Sliding-Mode Control

Before we design the DRSMC in Fig. 2, we need to discuss the continuous SMC first. Thus, we compute the error dynamics between (9.a) and (10.a) as follows:

$$\dot{e}(t) = Ae(t) + B\left(u_c(t) - u_{mc}(t)\right) + d(x(t), t) \qquad (20)$$

where $e(t) = x(t) - x_m(t)$. We assume $u_c(t)$ is defined as

$$u_c(t) = u_{mc}(t) - K_{c2}e(t) + \eta_c(t) \qquad (21)$$

where $K_{c2} = \beta_1^{-1}[\,\alpha_1\ \alpha_2\,]$ and $\eta_c(t)$ will be determined later. Thus, substituting (21) into (20), we have

$$\dot{e}(t) = \bar{A}e(t) + B\eta_c(t) + d(x(t), t). \qquad (22)$$

Due to $K_{c2} = K_{mc2}$, one can compute $\bar{A} = A - BK_{c2} = A - BK_{mc2}$. Next, we design the sliding mode function as follows:

$$s(t) = C_s e(t) + \int_0^t \left(-C_s\bar{A}e(\tau) + K_{c1}e(\tau)\right)d\tau \qquad (23)$$

where $C_s = B^{\dagger}$, and $K_{c1}$ is the controller gain. Differentiate (23), and then one has

$$\begin{aligned}\dot{s}(t) &= C_s\left(\bar{A}e(t) + B\eta_c(t) + d(x(t), t)\right)\\ &\quad - C_s\bar{A}e(t) + K_{c1}e(t)\\ &= \eta_c(t) + C_s d(x(t), t) + K_{c1}e(t).\end{aligned} \qquad (24)$$

When the controlled is able to enter the sliding manifold (i.e., $s(t) = \dot{s}(t) = 0$), one can get the equivalent $\eta_c(t)$ in the sliding manifold denoted as

$$\eta_{ceq}(t) = -C_s d(x(t), t) - K_{c1}e(t). \qquad (25)$$

Substituting (25) into (22), one can have the error dynamics in the sliding manifold

$$\dot{e}(t) = \bar{A}e(t) + B\eta_c^*(t) \qquad (26)$$

where $\eta_c^*(t) = -K_{c1}e(t)$. To efficiently suppress the match disturbances, one designs the controller gain $K_{c1}$ with LQAT [24]. To minimize the tracking error between system output and model system output, the following cost function is selected:

$$J = \frac{1}{2}\int_0^{t_{end}} \left\{e_y(\tau)^T Q_y e_y(\tau) + \eta_c^{*T}(\tau) R_y \eta_c^*(\tau)\right\} d\tau \qquad (27)$$

where $e_y(t) = y(t) - y_m(t)$, $Q_y = 10^q I_p$, $q \geq 0$, is a positive definite or a positive semidefinite real symmetric matrix and $R_y$ is a positive define matrix and invertible. As mentioned above, to calculate the gain of $K_{c1}$ the Riccati equation is given as

$$\bar{A}^T P + P\bar{A} - PB{R_y}^{-1}B^T P + C^T Q_y C = 0_n \qquad (28)$$

where $P$ is a positive symmetric define matrix satisfying the Riccati (28). Hence, the feedback gain can be calculated as $K_{c1} = R_y^{-1}B^T P$.

In addition, the controller gain $K_{c1}$ can also be calculated by using the following performance index:

$$\bar{A}^T\bar{P} + \bar{P}\bar{A} - \bar{P}B\bar{R}_y^{-1}B^T\bar{P} + \bar{Q}_y = 0_n \qquad (29)$$

where $\bar{Q}_y = \begin{bmatrix}\bar{Q}_{y_1} & 0\\ 0 & \bar{Q}_{y_2}\end{bmatrix}$ and $\bar{P}$ is a positive define matrix, which is solved by the Riccati (29). According to (29), it reveals that by selecting different weighting matrices $\bar{Q}_{y_1}$ and $\bar{Q}_{y_2}$, the different performance can be achieved. Generally speaking, with emphasis on the performance of the tracking error $e_y(t)$, the weighting matrix $\bar{Q}_{y_1}$ can be selected larger than the weighting matrix $\bar{Q}_{y_2}$.

Now, to guarantee the existence of sliding manifold, $\eta_c(t)$ proposed in SMC law (25) can be designed as

$$\eta_c(t) = -K_{c1}e(t) + u_{\pm}(t) \qquad (30)$$

where $u_{\pm}(t) = -\gamma_1 s(t) - (\gamma_2 + \gamma_3)\mathrm{sgn}(s(t))$, $\gamma_2$ and $\gamma_3$ are positive parameters. Substituting (30) into (24), one can get

$$\dot{s}(t) = C_s d(x(t), t) - \gamma_1 s(t) - (\gamma_2 + \gamma_3)\mathrm{sgn}(s(t)). \qquad (31)$$

*Theorem 1:* To guarantee the existence of the sliding manifold, the following Theorem 1 is introduced.

If the controller $u_c(t)$is designed as (21) with (30), one can ensure $\lim_{t\to\infty} s(t) = 0$ as well as $\lim\limits_{t\to\infty} \dot{s}(t) = 0$.

*Proof:* The Lyapunov function is selected as

$$V(s(t)) = \frac{1}{2}s^2(t). \qquad (32)$$

Differentiate $V(s(t))$, one has

$$\begin{aligned}\dot{V}(s(t)) &= s(t)\dot{s}(t)\\ &= s(t)(C_s(Ae(t) + B\left(u_c(t) - u_{mc}(t)\right) + d(x(t), t))\\ &\quad - C_s\bar{A}e(t) + K_{c1}e(t)).\end{aligned} \qquad (33)$$

Substituting $u_c(t)$ (21) into (33), one has

$$\begin{aligned}\dot{V}(s(t)) &= s(t)(C_s d(x(t), t) - \gamma_1 s(t) - (\gamma_2 + \gamma_3)\mathrm{sgn}(s(t)))\\ &\leq \|C_s\|\,\lambda_1\,\|x(t)\|\,|s(t)| - \gamma_1 s^2(t) - (\gamma_2 + \gamma_3)\,|s(t)|\,.\end{aligned} \qquad (34)$$

By designing $\gamma_3 = \|C_s\|\lambda_1\|x(t)\|$, one has

$$\dot{V}(s(t)) \leq -\gamma_1 s^2(t) - \gamma_2\,|s(t)| \leq 0 \qquad (35)$$

where $\gamma_1 > 0$ and $\gamma_2 > 0$. According to the Lyapunov theory, one ensures $\lim_{t\to\infty} V(s(t)) = 0$ as well as $\lim_{t\to\infty} s(t) = \lim_{t\to\infty} \dot{s}(t) = 0$ Therefore, the sliding manifold is guaranteed. □

### B. Digital Redesign of the Improved Continuous-Time $H_2$ Sliding-Mode Controller Design

After we prove the controlled error dynamics can reach the sliding manifold, we still need to prove the sliding mode function can satisfy the hitting condition in the discrete-time domain. Thus, according to the following Lemma 1, we can ensure the sliding mode function reaches the sliding manifold in the discrete-time domain.

*Lemma 1 [19]:* The following reaching condition is considered.

For $s(kT_s) > 0$, $\Delta s(kT_s) \leq -\gamma_1 T_s s(kT_s) - \gamma_2 T_s \text{sgn}(s(kT_s))$

for $s(kT_s) < 0$, $\Delta s(kT_s) \geq -\gamma_1 T_s s(kT_s) - \gamma_2 T_s \text{sgn}(s(kT_s))$

where $\Delta s(kT_s) = s(kT_s + T_s) - s(kT_s)$ and $T_s$ is sampling time and $k = 0, 1, \cdots, \infty$. If the above reaching conditions of the sliding motion are satisfied, then the trajectories of the error dynamic system (22) converge to the sliding mode function $s(kT_s) = 0$.

To prove the existence of sliding manifold in the discrete-time domain, we discretize (31) with Euler method [25], then one has

$$\begin{aligned} s(kT_s + T_s) &= s(kT_s) + T_s(C_s d(x(kT_s), kT_s) \\ &\quad - \gamma_1 s(kT_s) - (\gamma_2 + \gamma_3)\text{sgn}(s(kT_s))). \end{aligned} \tag{36}$$

According to Lemma 1 and $\gamma_3 = \|C_s\|\lambda_1\|x(t)\|$, so one can get

for $s(kT_s) < 0$

$$\begin{aligned} \Delta s(kT_s) &= -\gamma_1 T_s s(kT_s) \\ &\quad + T_s(C_s d(x(kT_s), kT_s) - (\gamma_2 + \gamma_3)\text{sgn}(s(kT_s))) \\ &\leq -\gamma_1 T_s s(kT_s) - \gamma_2 T_s \text{sgn}(s(kT_s)). \end{aligned}$$

For $s(kT_s) < 0$

$$\begin{aligned} \Delta s(kT_s) &= -\gamma_1 T_s s(kT_s) \\ &\quad + T_s(C_s d(x(kT_s), kT_s) - (\gamma_2 + \gamma_3)\text{sgn}(s(kT_s))) \\ &\geq -\gamma_1 T_s s(kT_s) - \gamma_2 T_s \text{sgn}(s(kT_s)). \end{aligned}$$

According to Lemma 1, it ensures that $s(kT_s)$ also reaches the sliding manifold in the discrete-time domain. When the sliding manifold is ensured, one has $\eta_c(t) = \eta_{ceq}(t)$in the sliding mode. Furthermore, we can rewrite (26) as

$$\begin{aligned} \dot{e}(t) &= \bar{A}e(t) - BK_{c1}e(t) \\ &= Ae(t) - B(K_{c1} + K_{c2})e(t) \\ &= Ae(t) + Bu_c^*(t), \end{aligned} \tag{37}$$

where $K_c = K_{c1} + K_{c2}$ and $u_c^*(t) = -K_c e(t)$. Then, (37) can be discretized as

$$e(kT_s + T_s) = Ge(kT_s) + Hu_d^*(kT_s) \tag{38}$$

where $G = e^{AT_s}$, $H = (G - I_n)A^{-1}B$. Using the digital redesign approach [21], the digital-redesign-based control law $u_d^* kT_s$ can be approached to

$$u_c^*(t) = u_d^*(kT_s) \cong u_c^*(kT_s + T_s), \text{for } kT_s \leq t < kT_s + T_s. \tag{39}$$

According to (39)

$$\begin{aligned} u_d^*(kT_s) &\cong u_c^*(kT_s + T_s) = -K_c e(kT_s + T_s) \\ &= -K_c(Ge(kT_s) + Hu_d^*(kT_s)). \end{aligned}$$

Then, $(I_m + K_c H)u_d^*(kT_s) = -K_c Ge(kT_s)$.

Thus, one has

$$u_d^*(kT_s) = -K_d e(kT_s) \tag{40}$$

where $K_d = (I_m + K_c H)^{-1} K_c G$.

After the control law is discretized, to implement the discrete-time SMC, one discretizes the sliding mode function (23) with the digital redesign technology as follows:

$$s(kT_s) = C_s e(kT_s) + s_I(kT_s) \tag{41}$$

$$s_I(kT_s + T_s) = s_I(kT_s) + T_s(-C_s\bar{A}e(kT_s) + K_{c1}e(kT_s)). \tag{42}$$

Besides, the continue time SMC-based control law (21) can be obtained as follow:

$$\begin{aligned} u_c(t) &= u_{mc}(t) - K_{c2}e(t) + \eta_c(t) \\ &= u_{mc}(t) - K_c e(t) - \gamma_1 s(t) - (\gamma_2 + \gamma_3)\text{sgn}(s(t)). \end{aligned} \tag{43}$$

By using the digital redesign method, the digital-redesign SMC-based control law can be obtained as

$$\begin{aligned} u_d(kT_s) &= u_{md}(kT_s) - K_d e(kT_s) - \gamma_1 s(kT_s) \\ &\quad - (\gamma_2 + \gamma_3)\text{sgn}\,(s(kT_s)) \end{aligned} \tag{44}$$

where $u_{md}(kT_s)$ is the digital-redesign control law of $u_{mc}(t)$. Using the digital redesign approach, the digital-redesign-based control law $u_{md}(kT_s)$ can be approached to

$u_{mc}(t) = u_{md}(kT_s) \cong u_{mc}(kT_s + T_s)$, for $kT_s \leq t < kT_s + T_s$.

Thus, one can have

$$\begin{aligned} u_{md}(kT_s) &\cong u_{mc}(kT_s + T_s) \\ &= -K_{mc}(Gx_m(kT_s) + Hu_{md}(kT_s)) \\ &\quad + E_{mc}r(kT_s + T_s) \\ &= (I + K_{mc}H)^{-1}\left[-K_{mc}Gx_m(kT_s)\right. \\ &\quad \left. + E_{mc}r(kT_s + T_s)\right]. \end{aligned} \tag{45}$$

Then, one can get

$$u_{md}(kT_s) = -K_{md}x_m(kT_s) + E_{md}r(kT_s + T_s) \tag{46}$$

where $K_{md} = (I_m + K_{mc}H)^{-1}K_{mc}G$ and $E_{md} = (I_m + K_{mc}H)^{-1}E_{mc}$. Therefore, we can obtain the HHMFC (44) based on digital-redesign SMC by

$$\begin{aligned} u_d(kT_s) &= -K_d e(kT_s) - K_{md}x(kT_s) + E_{md}r(kT_s + T_s) \\ &\quad - \gamma_1 s(kT_s) - (\gamma_2 + \gamma_3)\text{sgn}\,(s(kT_s)). \end{aligned} \tag{47}$$

To avoid chattering results from the nonlinear sign function in (47), the following Lemma 2 is given.

*Lemma 2 [19]:* To avoid the chattering phenomenon, one can replace the sign function with the saturation function. The saturation function is defined as

$\text{sat}(s(t)) = \frac{s(t)}{|s(t)|+\varepsilon}$, where $\varepsilon$ is an arbitrary and small positive constant. □

Since the saturation function is utilized, the digital-redesign SMC-based control law $\mu_d(KT_s)$ can be rewritten as

$$\begin{aligned} u_d(kT_s) &= -K_d e(kT_s) - K_{md}x(kT_s) + E_{md}r(kT_s + T_s) \\ &\quad - \gamma_1 s(kT_s) - (\gamma_2 + \gamma_3)\text{sat}\,(s(kT_s)). \end{aligned} \tag{48}$$

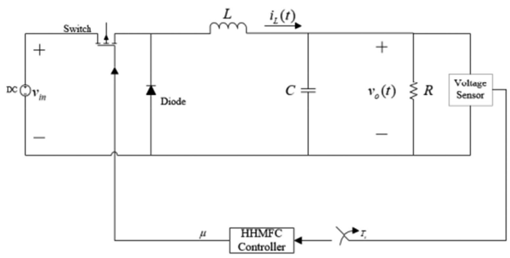


Fig. 3. Control architecture of the buck converter.

TABLE I
PARAMETERS OF BUCK CONVERTER

| Parameter names | Parameters | Values |
|---|---|---|
| Input voltage | $v_{in_0}$ | 30 (V) |
| Reference output voltage | $v_{ref}$ | 15 (V) |
| Inductor | $L_0$ | 10 (mH) |
| Capacity | $C_0$ | 1000 ( μF ) |
| Load resistance | $R_0$ | 100 ( Ω ) |

Now, we use the control law (48) to determine that the switch $\mu$ is ON or OFF. In the following, we use the function (48) to decide the switch $\mu$

$$\mu = \begin{cases} 1, \text{ when } u_d(kT_s) > 0 \\ 0, \text{ when } u_d(kT_s) \le 0 \end{cases}. \tag{49}$$

Therefore, a complete control structure to control the buck converter with the proposed HHMFC is shown in Fig. 3. And then, we discuss the results and analysis by Simulink and experiment in the following section.

## V. SIMULATION AND EXPERIMENT RESULTS

In this section, we demonstrate the performance of the buck converter with the proposed hybrid model following control based on digital-redesign sliding-mode control. Both the Simulink simulation and circuit experiments are considered. To highlight the contribution of the proposed HHMFC design, we compare the control performances with the second-order sliding mode control (SOSM) [3], [5] and the traditional proportional-integral-derivative (PID). The PID controller is designed as follows:

$$u(k) = k_p e_{pid}(k) - k_i \sum_{i=0}^{k} e_{pid}(i) - k_d \left[e_{pid}(k) - e_{pid}(k-1)\right] \tag{50}$$

where $e_{pid}(k) = v_o(kT_s) - v_{ref}$, $k_p$, $k_i$, and $k_d$ are self-adjusting parameters. According to [3] and [5], one can know the SOSM control is designed as

$$U = -\beta_2 \operatorname{sign}(\lceil \dot{s_e} \rfloor^2 + \beta_1 s_e) \tag{51}$$

where $s_e = v_o - v_{ref}$, and $\lceil \dot{s_e} \rfloor^2 = |\dot{s_e}|^2 \ \operatorname{sign}(\dot{s}_e)$. The SOSM controller determines the control input by

$$\mu = \begin{cases} 1, & \text{when } \lceil \dot{s_e} \rfloor^2 + \beta_1 s_e < -\lambda \\ 0, & \text{when } \lceil \dot{s_e} \rfloor^2 + \beta_1 s_e > \lambda \\ \text{unchanged}, & \text{otherwise} \end{cases}, \tag{52}$$

where $\lambda$ is a small constant. If the parameter $\beta_2 = 1$ is selected, the controller (46) becomes $U = -\operatorname{sign}(\lceil \dot{s_e} \rfloor^2 + \beta_1 s_e)$ which is the same as the controller proposed in [3].

In the following Section V-A, by using the Simulink tool, we implement the controllers with three control methods, which are the proposed HHMFC, the SOSM controller [3], and the traditional PID controller, to control the buck converter. Then comparisons are given. In Section V-B, we focus on the circuit realization of the HHMFC controller and the analysis of the experimental results is included.

### A. Simulink Simulation Results and Analysis

Now we use the MATLAB/Simulink to simulate the buck converter with the proposed HHMFC controller. And then, we compare the performances obtained with the HHMFC, PID controller, and SOSM controller, respectively. To have an effective comparison, we will change the load resistance at 0.25 s and the descent rate of the load resistance, which are 50% and 90%, respectively. Thus, we can contrast the stability of the three controllers.

First, referred to paper [3], in this article, one chooses the parameters of the buck converter in Table I. The sampling time $T_s$ is 0.00005 (s). Next, we define the HHMFC controller parameters. According to (10.a) and (10.b), we have $A = \begin{bmatrix} 0 & 1 \\ -10^5 & -10 \end{bmatrix}$, $B = \begin{bmatrix} 0 \\ 3 \times 10^6 \end{bmatrix}$ and $C = \begin{bmatrix} 1 & 0 \end{bmatrix}$.

For the system (10.a) and (10.b), the weighting matrices are selected $Q_y = \begin{bmatrix} 10^4 & 0 \\ 0 & 10 \end{bmatrix}$ and $R_y = 1$ to have $K_{c1} = \begin{bmatrix} 100 & 3.1623 \end{bmatrix}$. Then, one can get the control gain $K_c = \begin{bmatrix} 99.9667 & 3.1623 \end{bmatrix}$ by adding $K_{c1}$ and $K_{c2}$, where $K_{c2} = \begin{bmatrix} -0.0333 & -3.333 \times 10^{-6} \end{bmatrix}$. For the model system (11.a) and (11.b), we design the feedback control gain $K_{mc} = \begin{bmatrix} 0.0733 & 0.00039667 \end{bmatrix}$ and the forward control gain $E_{mc} = [0.1067]$ with the pole-placement technology. Due to the sampling time selected $T_s = 5 \times 10^{-5}$(s), one can perform the digital redesign with (38), (40), and (46), and we discretize $A$, $B$, $K_c$, $K_{mc}$, and $E_{mc}$ to have $G = \begin{bmatrix} 0.9999 & 4.9985 \times 10^{-5} \\ -4.9985 & 0.9994 \end{bmatrix}$, $H = \begin{bmatrix} 0.0037 & 149.9563 \end{bmatrix}^T$, $K_d = \begin{bmatrix} 0.1769 & 0.0067 \end{bmatrix}$, $E_{md} = [0.1007]$, and $K_{md} = \begin{bmatrix} 0.0673 & 3.7752 \times 10^{-4} \end{bmatrix}$. The initial conditions of (10.a) and (11.a) are given by $x(0) = \begin{bmatrix} 0 & 0 \end{bmatrix}^T$ and $x_m(0) = \begin{bmatrix} 15 & 0 \end{bmatrix}^T$. When the descent rate of the load resistance is 50%, the controller parameters are given by $\gamma_1 = 0.5, \gamma_2 = 0.95, \lambda_1 = 1$, and $\varepsilon = 0.057$. For the descent rate of the load resistance is 90%, the controller parameters are given by $\gamma_1 = 0.5$, $\gamma_2 = 0.95$, $\lambda_1 = 1$, and $\varepsilon = 0.057$. The reference trajectory is given by $r(t) = 15$. We choose the PID controller parameters as $k_p = 5$, $k_i = 0.00005$, and $k_d = 400$. Referred to [3], in this article, the SOSM controller parameters are chosen as $\beta_1 = 5 \times 10^4$, $\beta_2 = 1$, and $\lambda = 1$.

In Fig. 4, one transfers the load resistance from 100 to 50 Ω. For the demonstration the robustness of the proposed HHMFC, we reduce the load resistance by 90%, which means that 100 to 10 Ω in Fig. 5. To compare the proposed controller with SOMC proposed in [3], the specifications including line regulation, load

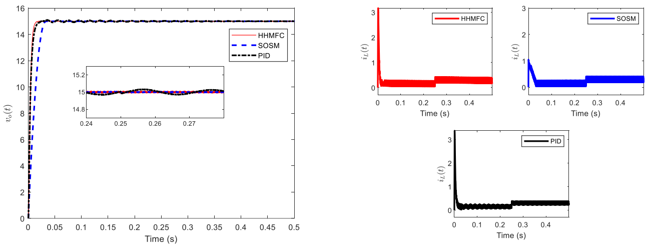


(a) (b)

Fig. 4. Performance of the buck converter when the load resistance transfer 100 to 50 Ω. (a) Output voltage of the buck converter. (b) Inductor current of the buck converter.

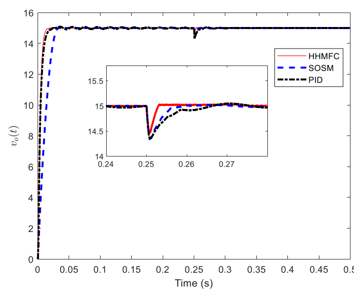


Fig. 5. Output voltage of the buck converter when the load resistance transfer $100$ to $10\,\Omega$.

TABLE II
SPECIFICATIONS OF BUCK CONVERTER

| | Line Regulation | Load Regulation | MOVD | MOVR |
|---|---|---|---|---|
| HHMFC | 0.008 % | 0.0667 % | 0.52 volt | 0.03 volt |
| SOSM [3] | 0.15 % | 0.0193 % | 0.65 volt | 0.02 volt |

regulation, the maximum output voltage drop (MOVD), and the maximum output voltage rise (MOVR) are given in Table II. The line regulation is computed when the input voltage is reduced from 30 to 20 V. By observing the responses in Figs. 4 and 5, it reveals that the proposed HHMFC with digital redesign SMC has better control performance. Using the HHMFC controller, the transient history is very short, and smooth and better robustness is obtained even if the load resistance value has variation. Furthermore, as shown in Table II, although the SOMC in [3] is with better load regulation performance, the proposed HHMFC controller has better performances of line regulation and MOVD. Thus, the HHMFC controller can suppress the disturbances efficiently with satisfactory performances than the SOMC [3].

## B. Experiment Results and Analysis

To implement the practical circuit, we use the Raspberry pi to realize the digital HHMFC controller. Raspberry pi is a Linux-based single-chip and has GPIO to connect other's circuits. One can receive the signals and output the signals through GPIO. However, the Raspberry pi can only receive digital signals, so one needs to have an analog-to-digital converter (ADC) to convert the analog continuous signals to digital discrete signals. After the calculation with the HHMFC built in the Raspberry pi, the HHMFC will output a high/low signal to control the MOSFET with GPIO. Since GPIO only can supply 3.3 (V) and it cannot switch on the MOSFET, we design a circuit to pull up the voltage such that when the Raspberry pi outputs a high signal, one can ensure that the MOSFET can be switched on successfully. The detailed component specification of the proposed buck converter is shown in Table III.

TABLE III
DETAILED COMPONENT SPECIFICATION OF THE PROPOSED BUCK CONVERTER

| Raspberry Pi | A/D converter | Switch device | High/Low side driver |
|---|---|---|---|
| Raspberry Pi 3 model B+ | MCP3008 | IRF540 | TLP250 |

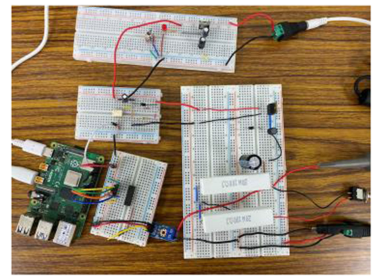

Fig. 6. Control circuit of the proposed HHMFC of buck converter.

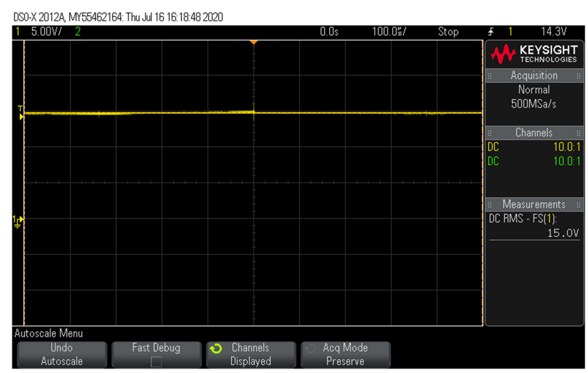


(a)

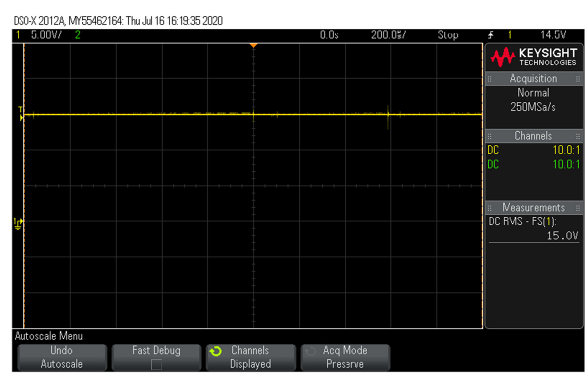


(b)

Fig. 7. Performance of the buck converter with the DRSMC controller. (a) Performance of the buck converter with the load resistance is $R = 100\,\Omega$. (b) Performance of the buck converter with the load resistance is $R = 50\,\Omega$.

Now we realize the HHMFC controller. The following designed matrix parameters are selected for realization. For the system (10.a) and (10.b), the weighting matrices are selected as $Q_y = 10^4$ and $R_y = 1$ to have $K_{c1} = [100\ 0.0082]$. Then, we can calculate the control gain $K_c = [99.9667\ 0.0082]$ by adding $K_{c1}$ and $K_{c2}$, where $K_{c2} = [-0.0333\ -3.333 \times 10^{-6}]$. For the model system (11.a) and (11.b), one designs the feedback control gain $K_{mc} = [0.0083\ 2.4667 \times 10^{-4}]$ and the forward control gain $E_{mc} = [0.0417]$. With $T_s = 5 \times 10^{-5}$(s), one can do the digital redesign with (40) and (46), and one discretizes $K_c$, $K_{mc}$, and $E_{mc}$ to have $K_d = [38.4476\ 0.0051]$, $K_{md} = [0.0068\ 2.3811 \times 10^{-4}]$, and $E_{md} = [0.0402]$. In this experiment, the controller parameters are given by $\gamma_1 = 9600, \gamma_2 = 75$ and $\varepsilon = 0.00001$.

Fig. 6 shows the complete structure of the buck converter. In Fig. 7(a) and (b), the results are obtained with the same buck converter circuit; while the load resistance is $100\,\Omega$, the measured output voltage is shown in Fig. 7(a), and then (b) shows the output voltage with the load resistance $50\,\Omega$. By observing the results, it reveals that when one changes the load resistance from 100 to $50\,\Omega$, the buck converter can still have good stability with the HHMFC.

## VI. Conclusion

In this article, a digital redesign technology was newly proposed by integrating with SMC. The design of hybrid $H_2$ model following control for the buck converter can be well completed by using the proposed digital redesign technology. It was verified that, by using the linear quadratic analog tracker, the states of the controlled systems can perfectly track the desired trajectory of the model systems. Through Simulink and the realized circuit experiment, we conclude the proposed HHMFC controller was with good robustness and the matched disturbances were efficiently suppressed by the proposed $H_2$ discrete sliding mode controller.

## References


[1] M. Sitbon, I. Aharon, M. Averbukh, D. Baimel, and M. Sassonker (Elkayam), “Disturbance observer based robust voltage control of photovoltaic generator interfaced by current mode buck converter,” *Energy Convers. Manage.*, vol. 209, Apr. 2020, Art. no. 112622.

[2] H. Li, Z. Guo, C. Liu, and T. Q. Zheng, “An extensible stability analysis method in time domain for cascaded DC-DC converters in electrical vehicles,” *Microelectron. Rel.*, vol. 88–90, pp. 1293–1299, Sep. 2018.

[3] S. Ding, W. X. J. Zheng, J. Sun, and J. Wang, “Second-order sliding-mode controller design and its implementation for buck converters,” *IEEE Trans. Ind. Inform.*, vol. 14, no. 5, pp. 1990–2000, May 2018.

[4] B. B. Naik and A. J. Mehta, “Sliding mode controller with modified sliding function for DC-DC buck converter,” *ISA Trans.*, vol. 70, pp. 279–287, Sep. 2017.

[5] L. Zang, Z. Wang, S. Li, S. Ding, and H. Du, “Universal finite-time observer based second-order sliding mode control for DC-DC buck converters with only output voltage measurement,” *J. Franklin Inst.*, vol. 357, pp. 11863–11879, 2019.

[6] K. Guesmi, N. Essounbouli, and A. Hamzaoui, “Systematic design approach of fuzzy PID stabilizer for DC–DC converters,” *Energy Convers. Manage.*, vol. 49, pp. 2880–2889, Oct. 2008.

[7] A. Benzaouia, F. Mesquine, H. Schulte, and S. Georg, “Stabilization of positive constrained T–S fuzzy systems: Application to a buck converter,” *J. Franklin Inst.*, vol. 351, pp. 4111–4123, Aug. 2014.

[8] T. K. Nizami and C. Mahanta, “An intelligent adaptive control of DC–DC buck converters,” *J. Franklin Inst.*, vol. 353, pp. 2588–2613, Aug. 2016.

[9] N. I. P. De León Puig, D. Bozalakov, L. Acho, L. Vandevelde, and J. Rodellar, “An adaptive–predictive control scheme with dynamic hysteresis modulation applied to a DC–DC buck converter,” *ISA Trans.*, vol. 105, pp. 204–255, 2020.

[10] T. K. Nizami, A. Chakravarty, and C. Mahanta, “Design and implementation of a neuro-adaptive backstepping controller for buck converter fed PMDC-motor,” *Control Engineer Pract.*, vol. 58, pp. 78–87, Jul. 2017.

[11] S. Skoczowski and S. Domek, “Robust model following control system,” *IFAC Proc. Volumes*, vol. 33, pp. 143–148, Sep. 2000.

[12] L. Zhao and S. Okubo, “A model following control system for nonlinear descriptor systems,” *Energy Procedia*, vol. 17, pp. 1724–1731, 2012.

[13] S. Das, M. S. Qureshi, and P. Swarnkar, “Design of integral sliding mode control for DC-DC converters,” *Mater. Today, Proc.*, vol. 5, pp. 4290–4298, 2018.

[14] I. F. Bouguenna, A. Azaiz, A. Tahour, and A. Larbaoui, “Robust neuro-fuzzy sliding mode control with extended state observer for an electric drive system,” *Energy*, vol. 169. pp. 1054–1063, Feb. 2019.

[15] L. Gracia, J. E. Solanes, P. Muñoz-Benavent, A. Esparza, J. V. Miro, and J. Tornero, “Cooperative transport tasks with robots using adaptive non-conventional sliding mode control,” *Control Eng. Pract.*, vol. 78, pp. 35–55, Sep. 2018.

[16] H. Du, X. Yu, M. Z. Q. Chen, and S. Li, “Chattering-free discrete-time sliding mode control,” *Automatica*, vol. 68, pp. 87–91, Jun. 2016.

[17] J. J. Yan, C. Y. Chen, and J. S. H. Tsai, “Hybrid chaos control of continuous unified chaotic systems using discrete rippling sliding mode control,” *Nonlinear Anal., Hybrid Syst.*, vol. 22, pp. 276–283, Nov. 2016.

[18] B. Rahmani, “Robust output feedback sliding mode control for uncertain discrete time systems,” *Nonlinear Anal., Hybrid Syst.*, vol. 24, pp. 83–99, May 2017.

[19] J. S. H. Tsai, J. S. Fang, J. J. Yan, M. C. Dai, S. M. Guo, and L. S. Shieh, “Hybrid robust discrete sliding mode control for generalized continuous chaotic systems subject to external disturbances,” *Nonlinear Anal., Hybrid Syst.*, vol. 29. pp. 74–84, Aug. 2018.

[20] S. Chakrabarty and A. Bartoszewicz, “Improved robustness and performance of discrete time sliding mode control systems,” *ISA Trans.*, vol. 65, pp. 143–149, Nov. 2016.

[21] S. M. Guo, L. S. Shieh, G. Chen, and C. F. Lin, “Effective chaotic orbit tracker: A prediction-based digital redesign approach,” *IEEE Trans. Circuits Syst. I, Fundam. Theory Appl.*, vol. 47, no. 11, pp. 1557–1569, Nov. 2000.

[22] X. Li, C. Wang, Q. Wen, X. Yu, and B. Wang, “Digital redesign of sliding mode control of LTI systems,” in *Proc. 6th World Congr. Intell. Control Autom.*, 2006, pp. 2431–2435.

[23] M. Singla, L. S. Shieh, G. Song, L. Xie, and Y. Zhang, “A new optimal sliding mode controller design using scalar sign function,” *ISA Trans.*, vol. 53, pp. 267–279, Mar. 2014.

[24] F. Ebrahimzadeh *et al.*, “A generalized optimal linear quadratic tracker with universal applications part 1 continuous time systems,” *Int. J. Syst. Sci.*, vol. 48, pp. 376–396, May 2016.

[25] S. Li, H. Du, and X. Yu, “Discrete-time terminal sliding mode control systems based on Euler’s discretization,” *IEEE Trans. Autom. Control*, vol. 59, no. 2, pp. 546–552, Feb. 2014.



**J. S. Fang** received the B.S. and M.S. degrees from the National Changhua University of Education, Taiwan, and the Ph.D. degree in electrical engineering from Cheng-Kung University, Taiwan, respectively.

His research interests include nonlinear control and intelligent algorithms.

**Sheng-Hong Tsai** received both M.S. and Ph.D. degrees in electrical engineering from the University of Houston, TX, USA, in 1985 and 1988, respectively.

Since August 1988, he has been an Associate Professor with Department of Electrical Engineering, National Cheng-Kung University, Taiwan. He has been a Full Professor since August 1992 and a Distinguished Professor since August 2002. His research interests include state-space self-tuning control, chaotic system control, partial differential system control, numerical analysis and robotics. He was (Executive) Editor for Science Development, published by National Science Council, Editor for Journal of the Chinese Institute of Electrical Engineering during, an Associate Editor for International Journal of Systems Science, and an Associate Editor for The Journal of The Franklin Institute.

**Jun-Juh Yan** received the M.S. degree in electrical engineering from National Central University, Taiwan, in 1992 and the B.S. and Ph.D. degrees in electrical engineering from the National Cheng Kung University, Taiwan, in 1987 and 1998, respectively.

At present, he is a Professor with the Department of Electronic Engineering, National Chin-Yi University of Technology, Taichung, Taiwan. His main research interests include the area of multirobot dynamic systems, chaotic systems, neural networks, variable-structure control systems, and adaptive control.

**P. L. Chen** received the B.S. degree in department of mechatronics engineering from the National Changhua University of Education, Taiwan, and the M.S. degree in electrical engineering from Cheng-Kung University, Taiwan, respectively.

His research interests include nonlinear control and sliding mode control.

**Shu-Mei Guo** (Member, IEEE) received the M.S. degree from the Department of Computer and Information Science, New Jersey Institute of Technology, Newark, in 1987 and the Ph.D. degree in computer and systems engineering from University of Houston, Houston, TX, USA, in May 2000.

Since June 2000, she has been an Assistant Professor with the Department of Computer System and Information Engineering, National Cheng-Kung University, Tainan, Taiwan, and since August 2010, she has been a Full Professor. Her research interests include various applications on evolutionary programming, chaos systems, Kalman filtering, fuzzy methodology, neural network, sampled-data systems, and computer and systems engineering.